
Non-Invasive point of care ECG signal detection and analytics for cardiac diseases

Bachelor of Technology

for the course

CL 499

by

Shubham Kumar Gupta

Roll No. 180107058

under the supervision of

Prof. Resmi Suresh

Prof. Dipankar Bandyopadhyay



to the

**DEPARTMENT OF CHEMICAL ENGINEERING
INDIAN INSTITUTE OF TECHNOLOGY GUWAHATI
GUWAHATI-781039, INDIA**

May 2022



INDIAN INSTITUTE OF TECHNOLOGY, GUWAHATI
Department of Chemical Engineering
Guwahati – 781039 (Assam)

CERTIFICATE

It is certified that the project work entitled "Non-Invasive point of care ECG signal detection and analytics for cardiac diseases" that is being submitted by **Mr. Shubham Kumar Gupta (Roll no. 180107058)**, is a bonafide work carried out under my supervision in the Department of Chemical Engineering, I.I.T. Guwahati and this work has not been submitted to any other institution or university for any degree.

Date:

Prof. Resmi Suresh

Department of Chemical Engineering
Indian Institute of Technology
Guwahati-781039, Assam, India

Prof. Dipankar Bandyopadhyay

Department of Chemical Engineering
Indian Institute of Technology
Guwahati-781039, Assam, India

ACKNOWLEDGEMENT

This undertaking would not have been feasible without the assistance of numerous individuals, all of whom are truly appreciated and heartily acknowledged for their contributions. I would like to take this opportunity to express my gratitude and indebtedness to **Prof. Reshmi Suresh** and **Prof. Dipankar Bandyopadhyay**, my project supervisor, for their enthusiasm, patience, insightful comments, useful information, practical advice, and never-ending ideas throughout this project, as well as for instilling in me a sense of research aptitude. I would want to convey my heartfelt appreciation to him for his unflinching support and assistance.

Shubham Kumar Gupta

Roll No. 180107058

Dept. of Chemical Eng.

I.I.T. Guwahati

Table of Contents

S No.	Title	Pg. No
1	Abstract	5
2	Nomenclature	6
3	Introduction	7
4	Theoretical background	9
4.1	Medical background	
4.2	Overview of an abnormal heart	
4.3	Conduction systems of the heart	
4.4	Electrical pathway of the heart	
4.5	Electrocardiogram (ECG)	
4.5.1	Morphology of the intervals of normal ECG	
5	Literature review	15
5.1	Steps to perform ECG	
5.2	Working principle of ECG	
5.3	Case Study: Sanket's 12 leads ECG	
5.4	Electrode & micropatterned electrodes	
5.5	Sample dataset	
6	Methodology	20
6.1	Objective	
6.2	Block diagram	
6.3	Sources of noise	
6.4	Circuit diagram & components	
6.5	Datapoints	
6.6	Redefining dataset	
6.7	Dataset modelling and architecture	
7	Results and discussion	28
8	Conclusions	32
9	Future Scope	
10	References	33

1. ABSTRACT

Cardiovascular disorders account for one in every three fatalities worldwide and are the major cause of death. In India, we have the world's highest cases of cardiovascular diseases. Annual cardiovascular disease deaths are predicted to grow from 2.26 million to 4.77 million in about 30 years of time span from 1990 to 2020. The prevalence of coronary heart disease in India has been studied for several decades and has ranged from 1.6 to 7.4 percent in rural areas and 1 percent to 13.2 percent in metropolitan areas. The existence of a number of risk factors, such as cigarette use, an unhealthy diet and obesity, physical inactivity and alcohol use, hypertension, diabetes, and a high cholesterol level, are all known to cause heart strokes and attacks. Cardiovascular problems can be detected using electrocardiograms (or ECG). This test is commonly used to diagnose heart illness, a heart attack, an enlarged heart, or abnormal heart rhythms, all of which can lead to heart failure. While there are traditional methods and devices for performing ECG, the setup is expensive, time-intensive, and requires a high level of awareness of how to execute and evaluate ECG. As generations change, there is a need for a portable, cost-effective, and self-predicting cardiovascular disease technology that can detect heart risks with minimal setup and understanding. When it comes to the improvement of heart health, it is never too late to adopt new technologies. The study discusses the most prevalent cardiovascular anomalies, analyses ECG waves and non-invasive ECG measuring techniques, and intends to design a device that can measure ECG signals non-invasively. Numerous case studies of currently available items on the market were analyzed and used to deduce constraints and techniques. The biosensors used in the manufacture of devices have been explored. Additionally, the study on "Atrial Fibrillation" identification is conducted using a single lead ECG dataset (a database of ECG amplitudes v/s time for persons aged 30-80 years). Using ECG measurements, a Convolutional Neural Network model is utilized to predict "Atrial Fibrillation." The study discovered that Convolutional Neural Networks were capable of accurately predicting the same with an 81.36% accuracy.

2. NOMENCLATURE

Symbol	Meaning	Units
ECG/EKG	Electrocardiogram	
Op-Amp	Operational Amplifier	
A.F.	Atrial Fibrillation	
CVD	Cardio Vascular Disease	
AV	Atrio Ventricular	
A.D.C.	Analog To Digital Converter	
CNN	Convolution Neural Network	
ANN	Artificial Neural Network	
G.P.S.	Global Positioning System	
μ	Dipole Moment	Debye
Φ	Potential at a position	Volt (V)
I	Current	Ampere (A)
V	Voltage	Volt (V)
T	Temperature	Kelvin (K)
R	Resistor	Ohm (Ω)
C	Capacitor	Micro farad (μF)
L	Inductor	Henry (H)
B.P.M.	Beats per minute	beats/m
aVL	augmented Vector Left	
aVR	augmented Vector Right	
aVF	augmented Vector Foot	
DC	Direct current	
AC	Alternating current	

3. INTRODUCTION

Ailments that impact the function of our hearts are referred to as heart disease. It could be caused by problems with the heart's blood supply, heart rate or rhythm, or defects in the cardiac artery's architecture. Heart disease kills about 17.5 million people each year, according to the World Health Organization (WHO) reports. It is essential to evaluate and recognize heart illness early to protect against sudden mortality as a result of heart attack or cardiac arrest. Cardiologists employ a sensor for the electrocardiogram (ECG) to quickly and without intervention detect abnormal heart rhythm and signs of likely heart disease.

The demand for value-added components has increased as smartphones and tablets have grown in popularity. The most common way to sell content for mobile devices has been to sell "apps" on online marketplaces. These are usually pure software add-ons that take advantage of the existing platform's hardware capabilities. These devices now come with high-resolution touch screens, accelerometers, G.P.S., and cellular and wireless data access as standard hardware. For general-purpose applications, these hardware interfaces provide a high-quality standard development environment. This set of hardware may not be sufficient for more specialized applications, but it does serve as an exemplary user interface, recording platform, and network uplink.

In today's environment, obtaining affordable healthcare is a challenge. As government organizations and private businesses look for ways to save money, there may be a market opportunity to utilize mobile device technology's widespread availability. In the future years, even emerging countries' capable low-end smartphone markets are likely to rise. Several physiological data sets could be helpful to the health business. One might, for example, have persistent symptoms that are difficult to replicate in a therapeutic environment.

Using the circulatory system, the heart removes carbon dioxide and wastes from the blood while providing oxygen and nutrition to the body's tissue. People who have a problem with their hearts can suffer from abnormal heartbeats that are either too rapid or too sluggish. Arrhythmia is the medical term for this condition. There are a number of valves, nodes, and chambers in the heart that control blood flow. There are different types of abnormal heartbeat; they are Atrial Fibrillation and Flutter, Congestive Heart Failure (CHF), Congestive (Dilated) Cardiomyopathy, Mitral Valve Prolapse, Hypertensive Heart Disease, Cardiogenic Shock, Dissection of the Aorta, Hypokalemia,

Hyperthyroidism, Anaphylaxis, Hypoglycemia (low blood sugar), Hypothyroidism, Aortic Coarctation, Ventricular Septal Defects. The abnormal heartbeat has various types. When an individual's heart rhythm is aberrant, this is referred to as abnormal cardiac rhythm. It occurs when an individual's heart's electrical system malfunctions or fails to perform properly. This could be an indication of undiagnosed coronary heart disease or another medical condition. Arrhythmias are caused by irritable cardiac cells, blocked signals, aberrant routes, medications and stimulants, and spasms of the coronary arteries. Electrocardiography is used to diagnose arrhythmias (ECG). The ECG demonstrates to the physician how the heart's electrical circuitry operates.

While individuals are occasionally aware of irregular cardiac rhythms, they frequently experience only their repercussions, such as weakness or fainting. Electrocardiography is used to determine the cause of the patient's heart condition. Treating an irregular heartbeat and preventing future episodes is the purpose of this therapy. In order to control the contraction of the cardiac muscle fibers, electrical current is carefully routed through the heart in a controlled manner. Each heartbeat is initiated by an electrical current generated by the heart's pacemaker (also known as the sinus node or sinoatrial node), which is located at the top of the upper right heart chamber (right atrium). The heart rate is determined by the rate at which the pacemaker discharges the electrical current. This pace is determined by nerve impulses and the blood level of specific hormones.

Convolution Neural Networks have been used to construct a predictive model for "Atrial Fibrillation" based on ECG data points from the "Physionet AliveCor's Short Single Lead ECG Recording" dataset. Normal and abnormal ECGs were included in the data collection, which had amplitude and time values for each ECG in ECG datasets; a single row appears to be an image matrix. A proposed answer to the problem of image categorization is the Convolution Neural Network model. When you feed an image into a Convolutional Neural Network (CNN), the algorithm assigns weights and biases (learnable) to different sections of the image and can tell them apart. ConvNets require less pre-processing than other classification techniques. While filters are hand-engineered in basic approaches, ConvNets have the potential to learn these filters/characteristics with enough training. ConvNet's architecture is inspired by visual cortex organization and is similar to human brain connectivity patterns. Individual neurons respond to stimuli in the Receptive Field, which is a part of the visual field. A set of these fields covers the full visual field.

4. THEORETICAL BACKGROUND

4.1 Medical Background

The heart is located in the center of our chest, between the lungs, slightly to the left of our breastbone, and in the middle of our chest, as seen in figure 1. (sternum). The pericardium, which resembles a sac, is a double-layered membrane that surrounds and protects your heart. The anterior pericardium is the outer layer of our heart's major blood vessels, which covers the roots of our heart's major blood arteries and is connected to the spinal column, diaphragm, and other parts of the body by ligaments. The cardiovascular system is made up of the heart and blood vessels. The heart functions as a pump, supplying blood to all of your body's organs, tissues, and cells. Blood is returned to the heart through veins. The heart is divided into four chambers: two upper (atria) and two lower (ventricles) (the ventricles). The heartbeat is the contraction of the heart muscle that happens during the process of blood pumping.

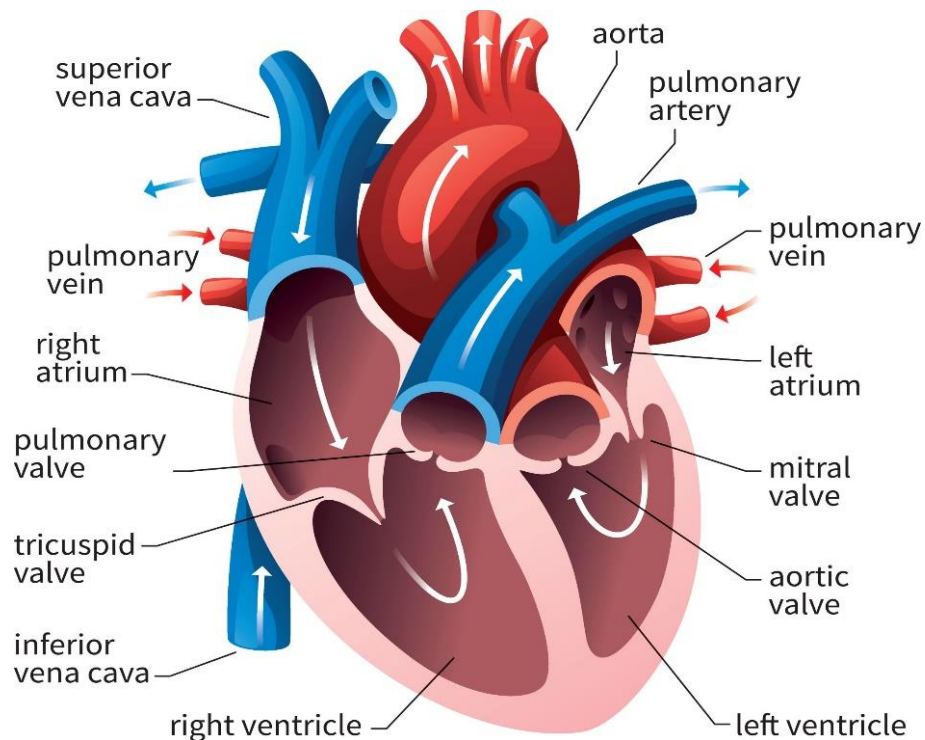


Figure 1 Anatomy of the heart; **Source:** Queensland Cardiovascular Group; **Description:** Here, figure 1 shows the labeled anatomy of the human heart and the blood flow in the four chambers and sections of the heart.

4.2 Overview of an Abnormal Heart

There is a total of four chambers in our heart, each having a specific role. Muscular walls in each chamber of the heart contract in a coordinated sequence, pumping blood as the body needs while expelling the least amount of energy feasible throughout each heartbeat. The most common cause of irregular cardiac rhythm is heart disease. While people are occasionally aware of irregular cardiac rhythms, they frequently only feel their repercussions, such as weakness or fainting. When an individual's heart rhythm is aberrant, this is referred to as abnormal cardiac rhythm. It occurs when an individual's heart's electrical system malfunctions or fails to perform properly. This could be an indication of undiagnosed coronary heart disease or another medical condition. Arrhythmias are caused by irritable cardiac cells, blocked signals, aberrant routes, medications and stimulants, and spasms of the coronary arteries. It is only when the heart rate is excessively rapid (referred to as tachycardia) or sluggish (referred to as bradycardia) that the cardiac rhythm is considered abnormal. Figure 2 denotes Atrial Fibrillation; figure 3 denotes tachycardia; figure 4 denotes Bradycardia.

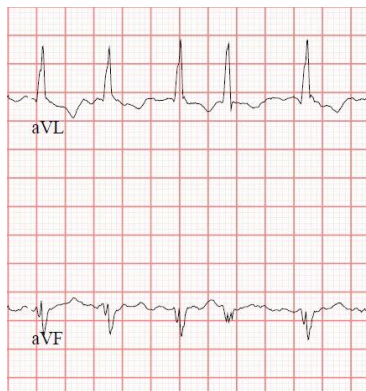


Figure 2 (a) Atrial fibrillation

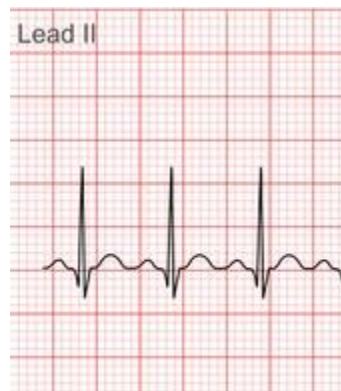


Figure 2 (b) Tachycardia



Figure 2 (c) Bradycardia

Source: stemlynsblog.org; **Description:** Here, figure 2 shows the recorded ECG waves of an abnormal heart, here figure 2(a) shows the ECG wave of Atrial fibrillation, figure 2(b) shows Tachycardia, and figure 2(c) shows Bradycardia

4.3 Conduction Systems

Contraction of the cardiac muscle fibers is regulated by electricity that passes precisely through the heart along different channels at a controlled rate. The heart's pacemaker (also known as the sinoatrial node) generates an electrical current that starts each heartbeat. It is located near the top of the upper right heart chamber (right atrium). The rate at which the pacemaker discharges the electrical current determines the heart rate. This pace is determined by nerve impulses and the blood level of specific hormones. The sympathetic and parasympathetic sub-divisions of the autonomic nervous system control the heart rate. The sympathetic division raises the heart rate via

a network of nerves known as the sympathetic plexus. . The parasympathetic division reduces the heart rate via a single nerve, the vagus nerve. Sympathetic hormones such as epinephrine (adrenaline) and norepinephrine, which are released into the bloodstream by the sympathetic division, also regulate heart rate (noradrenaline). This sympathetic division promotes an increase in heart rate. Thyroid hormone, which is secreted into the bloodstream by the thyroid gland, raises heart rate. An adult's resting heart rate should be between 60 and 100 beats per minute. Adolescents and young adults, particularly those who are physically fit, may have lower rates. An individual's heart rate normally varies in response to exercise and other stimuli such as pain and anger. Figure 3 depicts our heart's conduction mechanism.

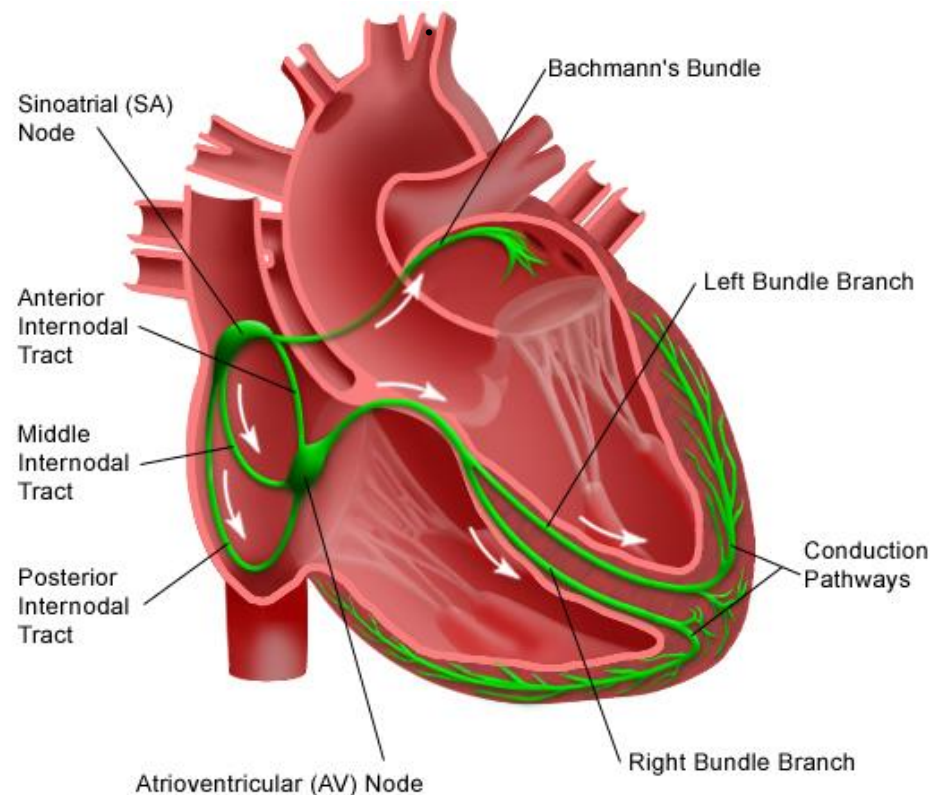


Figure 3 Conduction System; **Source:** H. Karam, E., Tashan, T., & F. Mohsin, E. (2019). Design of Model Free Sliding Mode Controller based on BBO Algorithm for Heart Rate Pacemaker. International Journal of Modern Education and Computer Science, **Description:** Here, figure 3 shows the labeled picture of the conduction system of the human heart, with branches and two important nodes SA node and AV node

4.4 Electrical Pathway

The sinoatrial (sinus) node is responsible for generating an electrical impulse that travels across the right and left atria, causing them to constrict and contract. When an electrical impulse reaches the atrioventricular node, it is slightly delayed in its arrival time. It descends the His bundle, which is separated into two branches: the right bundle branch, which leads to the right ventricle, and the left bundle branch, which leads to the left ventricle. It subsequently spreads to the ventricles,

constricting them. Electrical current travels along with the bundle of His after it has passed through the atrioventricular node. Right, and left ventricular bundles are formed by a bundle of His, which is a cluster of fibrous tissue. Starting at the bottom, it travels throughout the ventricle's surface, squeezing them and causing blood to be evacuated from the body. Figure 6 shows the electrical pathway of our heart.

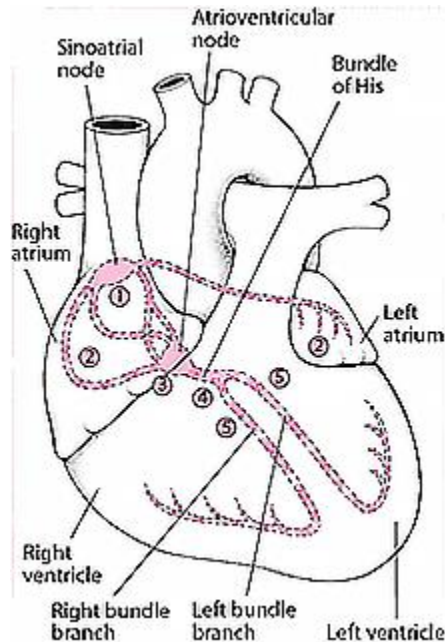


Figure 4 Electrical pathway; **Source:** Marriott, H. J. (1964). *Electrocardiographic abnormalities, conduction disorders, and arrhythmias in primary myocardial disease*; **Description:** Here, Figure 4 shows the labeled diagram of the electrical pathway present inside the human heart.

4.5 Electrocardiogram (ECG)

The heart's electrical signals are shown graphically in this diagram. In 1983, Willem Einthoven is the first person to utilize an electrocardiogram (ECG). The ECG is made up of three main signal components. Certain diseases may cause an abnormal heartbeat, which may indicate the presence of an arrhythmia by altering one of these traces. Using electrodes, the ECG records the heart's electrical activity by putting electrodes (up to 12 electrodes) at various points on the body. It's well accepted that the automation of cardiac arrhythmias using ECG is an essential area of study in today's medical community. Electrocardiography (ECG) and Tilt Tests are used to diagnose arrhythmias. The ECG demonstrates to the physician how the heart's electrical circuitry operates. Tilt tests inform the physician whether or not various body positions will cause an arrhythmia. They are effective for examining the hearts of individuals who have unexplained fainting. Electrocardiography is used to make the diagnosis. The treatment goal is to restore the heart's normal rhythm and prevent future episodes. It is drawn on a special form of graph paper in which

1mm corresponds to 0.04s on the x-axis and 0.1mV on the y-axis. On the right side of the graph paper is a square wave pulse symbol representing the calibration level, where a peak equals two square boxes, i.e., a 1mV signal represents a 10mm deflection. An ECG recording contains a total of 12 leads; six limb leads(3 limb leads and three augmented leads) are labeled as Lead I, II, III, aVF, aVR, aVL, and six chest leads are labeled as V1, V2, V3, V4, V5, V6. Sample ECG is shown in figure 7.

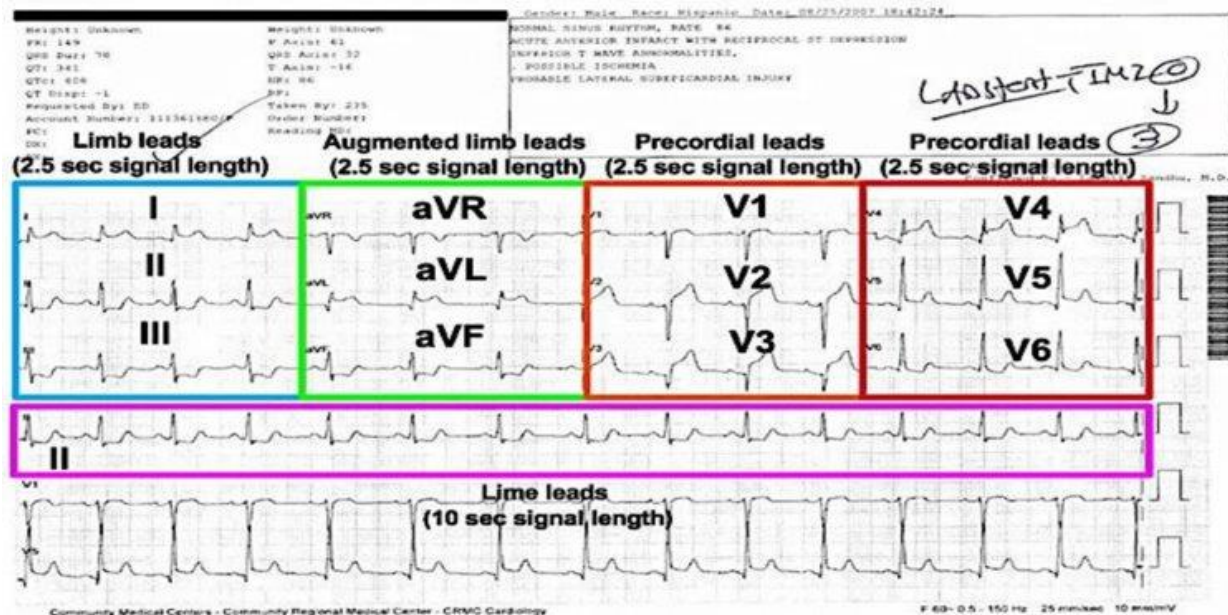


Figure 5 A Sample Recorded Electrocardiogram;
Source: ECGlibrary.com; **Description:** This figure shows the recorded electrogram of a person; here, it shows different sections of the recorded leads.

4.5.1 Morphology of the intervals of Normal ECG

When we analyze an ECG wave, we can see that it is composed of discrete segments. ECG waves and intervals are classified as P-wave, PR interval, P.R. segment, Q.R.S. Complex, J-wave, ST segment, T-wave, and U-wave. Traditionally, ECG interpretation begins with the P-wave. The P wave indicates atrial depolarization (activation). The P.R. interval is the time between the commencement of the P-wave and the onset of the Q.R.S. complex. The PR interval is used to determine whether or not impulse conduction from the atria to the ventricles is normal. At the end of the P-wave and the start of the Q.R.S. complex, there is a flat line called the P.R. Segment. In the atrioventricular node, it likewise shows sluggish impulse conduction. The PR segment acts as the ECG curve's starting point (referred to as the reference line). By comparing any deflection/amplitude wave to the P.R. section, any deflection/amplitude wave can be determined. The Q.R.S. complex represents the depolarizing ventricles (activating). The "Q.R.S. complex" is constantly referred to, even if all three waves are not always present. The Q.R.S. complex is a reflection of left ventricular depolarization because the electrical vector generated by the left

ventricle is many times bigger than the electrical vector generated by the right ventricle. The ST-Segment corresponds to the action potential's plateau phase (phase 2). The S.T. segment must always be examined because it is altered under a variety of settings. Numerous situations result in fairly distinctive ST-segment alterations. The S.T. segment is particularly relevant in acute myocardial ischemia because ischemia results in ST-segment deviation. The magnitude of depression/elevation is expressed as the height difference between the J point and the P.R. segment. The J point denotes the commencement of the S.T. segment. The T-wave indicates contractile cells' rapid repolarization (phase 3), and T-wave alterations occur under a wide variety of situations. U-wave is a positive wave that occurs immediately following the T-wave. Its amplitude is typically one-fourth that of the T-wave. Figure 8 illustrates the shape of various segments of an ECG wave.

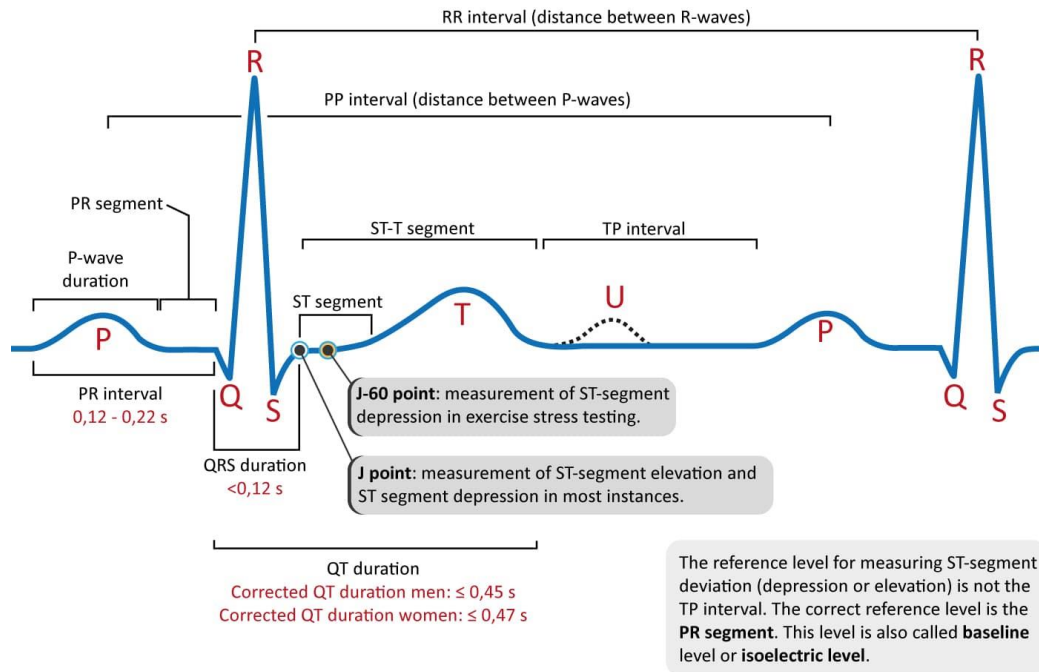


Figure 6 Morphology of an ECG wave; **Source:** H. Karam, E., Tashan, T., & F. Mohsin, E. (2019). Design of Model Free Sliding Mode Controller based on BBO Algorithm for Heart Rate Pacemaker. International Journal of Modern Education; **Description:** This figure shows the labeling of the different sections of an ECG wave

4.6 Convolution Neural Network (CNN)

Convolutional Neural Networks have made substantial progress in a range of fields connected to pattern identification during the last decade, ranging from image processing to speech recognition. The most significant advantage of CNNs is the reduction in the number of parameters required by ANNs. With this success, researchers and developers are rethinking the use of conventional ANNs in order to execute complex tasks that were previously beyond their capabilities. An essential principle is that CNN problems should not be spatially dependent in any way whatsoever. All that counts is that the objects are spotted, no matter where they appear in the images. Abstract characteristics are another important aspect of CNN. In

picture classification, for example, the edge may be identified first, followed by simpler shapes in the second layer, and lastly by higher-level attributes in the subsequent layers. Figure 9 shows how CNN works.

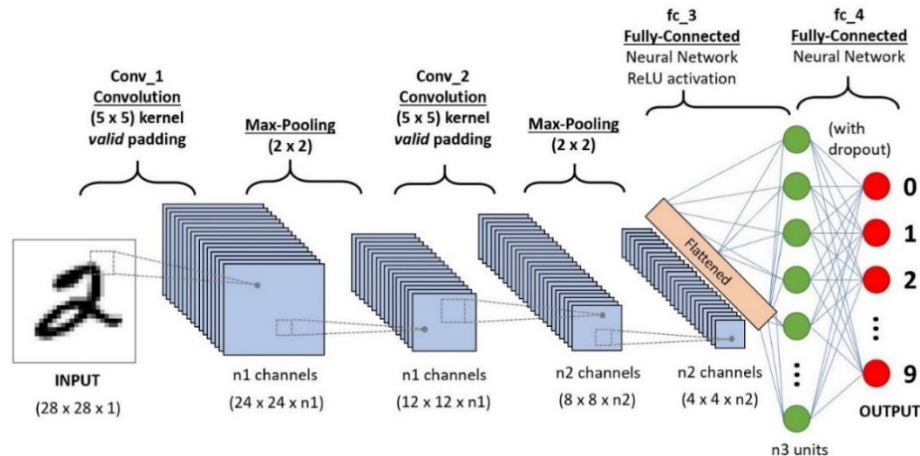


Figure 7 Convolution Neural Network; **Source:** towardsdatascience.com;
Description: This figure shows the example of how a convolution neural network works on a mnist hand written dataset, in mid its showing hidden layers, methods applied and neural networks output

5. LITERATURE REVIEW

5.1 Steps to Perform ECG

An ECG can be performed in a variety of methods. The test is generally performed by attaching a series of small, adhesive sensors called electrodes to your arms, legs, and chest. These are attached to an ECG recording machine via wires. These are the steps necessary to record an individual's ECG using the traditional approach. The below figures show the position of ECG electrodes. The following are the processes involved in recording an ECG of a person using the traditional method:

- To perform an ECG with 12 leads, electrodes are placed over the body.
- Despite the name 12 leads ECG, it only uses ten electrodes. Certain electrodes are connected in pairs, providing two leads.
- Electrodes are typically self-adhesive pads filled with a conducting gel. The electrodes are attached through snap-on connectors to the electrocardiograph or heart monitor's cables.
- ECG Gel enhances conductivity between the skin and the electrodes of the heart rate monitor.
- The ECG's twelve leads reflect twelve electrical images of the heart from twelve different angles. The standard 12 leads method comprises the placement of 10 electrodes on the body: one on each leg and six across the chest.
- The six limb leads, which are acquired from three electrodes attached to the right arm, left arm, and left leg, stare vertically at heart.
- The earth electrode is located on the right leg.

- The ECG machine uses the negative pole as a zero reference, while the positive pole serves as the "point of view," and the line linking the two poles serves as the "line of sight."

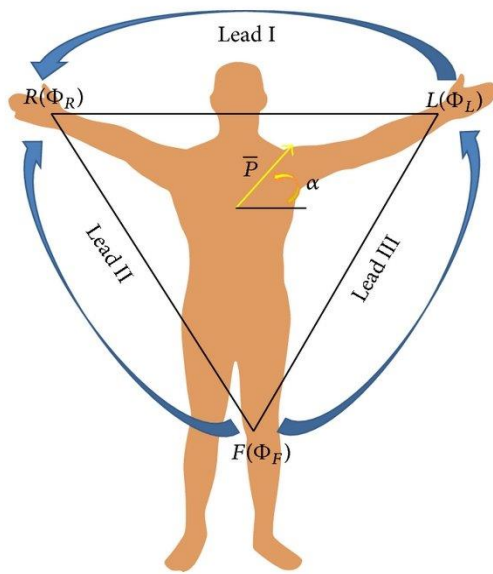


Figure 8 Limb Leads; **Source:** Haider, A., & Fazel-Rezai, R. (2014). Heart Signal Abnormality Detection Using Artificial Neural Networks1. Journal of Medical Devices; **Description:** This figure shows the Einthoven's triangle showing how the leads vector are interlinked as a vector

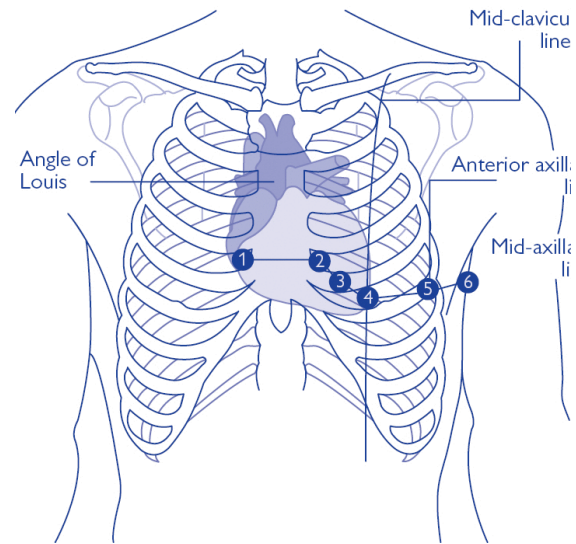


Figure 9 Chest Leads; **Source:** Camm, A. J., Lüscher, T. F., Maurer, G., & Serruys, P. W. (Eds.). (2018). ESC CardioMed; **Description:** This figure shows the labeled diagram of the chest showing six chest leads position

5.2 Working Principle of ECG

It is based on the principle that when a muscle contracts, a little electric current is generated that may be detected and measured using electrodes positioned appropriately on the body. A resting electrocardiogram requires the subject to lie in the resting position, with electrodes put on the arms, legs, and six locations on the chest above the heart area. The electrodes are adhered to the subject's skin using a specific lubricant. The electrode detects and transmits the current to an amplifier located inside the electrocardiograph. The electrocardiograph then intensifies the current and records it as a wavy line on paper. A sensitive lever records variations in current on a moving sheet of paper in an electrocardiograph. Additionally, a modern electrocardiograph can be connected to an oscilloscope, a device that displays current on a screen. If the Φ symbol is used to denote potentials at different regions, then, on completing the circuit by touching the Left and Right thumbs or arms, we can get Lead I; similarly, using Foot and Right-arm, we can get Lead II and so on.

$$\text{Lead I: } V_I = \Phi_L - \Phi_R \quad (1)$$

$$\text{Lead II: } V_{II} = \Phi_F - \Phi_R \quad (2)$$

$$\text{Lead III: } V_{III} = \Phi_F - \Phi_L \quad (3)$$

$$aVF = \Phi_F - \frac{\Phi_L + \Phi_R}{2} \quad (4)$$

$$aVL = \Phi_L - \frac{\Phi_F + \Phi_R}{2} \quad (5)$$

$$aVR = \Phi_R - \frac{\Phi_F + \Phi_L}{2} \quad (6)$$

$$\text{Cardiac Axis} = \pm \tan^{-1}\left(\frac{aVF}{V_I}\right) \quad (vii) \quad (7)$$

5.3 Case Study: Sanket's 12 leads ECG

Sanket's 12 leads (figure 10) ECG is an Indian firm Sanket's ECG recording device that has been widely used in rural markets with the assistance of physician's teams to record ECGs in an easier and less expensive manner without the need for additional electrode implantation. This is a little gadget that may be placed on various regions of the body sequentially to capture the person's ECG. It's a little complicated, and it's probably only possible to perform an ECG with the assistance of a qualified someone who understands which two points on the body correspond to which ECG leads. This is a versatile item that may be utilized anywhere and at any time. If the device is misplaced, there may be complications with the reading of the ECG, which can also result in inaccuracies. It has a total of 2 electrode systems, which are touched at different body parts using electrodes to get a single lead ECG; completing different circuits, we can get all 12 leads ECG using it; below is the figure of Sanket's 12 leads portal ECG and the circuit diagram of the device.



Figure 10 Sanket's 12 leads ECG,
Source: mashelkarfoundation.org,
Description: This figure shows
 this sanket's ECG device

5.4 Electrode & Micropatterned Electrodes

Electrical systems perceive (measure) or stimulate (induce) electrical potentials within cells passively or actively and serve as a link between biological structures and electronic systems. Our bodies generate ionic potentials, which must be converted to electronic potentials before they can be detected. Electrodes are devices that convert ionic potential to electrical potential. The Bio Electrode is the transducer that converts the ionic body current to the electronic current flowing through the electrode. It can conduct even extremely modest currents through the interface between the body and the electronic measuring circuit. When the current flows from the electrode to the electrolyte, oxidation is predominant; when the current flows in the opposite direction, the reduction is dominant. The electrodes are constructed of an Ag/AgCl disc encased in conductive gel and have a resistance of around 100 m. The diameter of the disc is approximately 25 mm, the diameter of the gel is approximately 16 mm, and the diameter of the Ag/AgCl disc is around 10 mm. A cross-sectional scan reveals that the gel beneath the tip is approximately 600 m thick but is significantly thicker in the remaining portion, making it impossible to calculate the electrode equivalent area. The gel enhances conductivity between the skin and the electrodes of the heart rate monitor. For Microelectrodes, detection of the physical stress at different parts of body, the polymer substrate is made of PDMS and the conducting material to coat the micro/nanopillars includes Aluminum or RGO. the computing processor process the voltage signal correlates it with the physical stress by receiving the voltage signal from the sensor arrangement corresponding to the body-potential comes out of a particular muscle of the body part; comparing the voltage signal's amplitude and frequency with respect to a reference value to detect physical stress of the body part whereby higher amplitude and frequency of the signal corresponds to a stressed condition of the muscle compared to relaxed situation; converting the voltage to a digital signal and transfers it with the detected physical stress wirelessly to the remote recipient including cooperative mobile application embodied in user's mobile phone for real-time display of the detected physical stress and the digital signal and/or storing data associated with the same for future analysis. Figure 11 shows micro pattern electrodes, and figure 12 shows gel electrodes, some electrodes that can be used are “Electrically conductive Silicone Rubber Sheet” or “Conductive Hook & Loop,” which have a resistivity of around 1.57 to $1.4\Omega/\text{in}^2$.

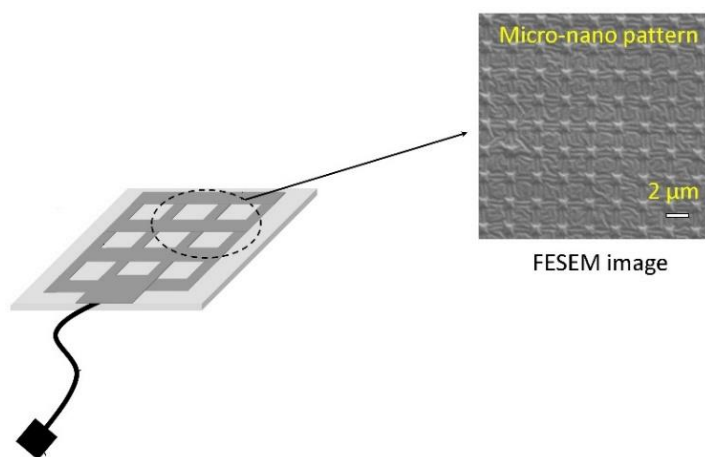


Figure 12 Micropatterned Electrodes; **Source:** Flexible Neural Electrode Array Based-on Porous Graphene for Cortical Microstimulation and Sensing. Scientific Reports; **Description:** This figure, shows a micropatterned electrode micro Field emission scanning electron microscopy (FESEM) image



Figure 11 Sticky Gel Electrodes, **Source:** Analysis of local corrosion of large metallic structures or reinforced concrete structures by electrochemical impedance spectroscopy; **Description:** This image shows a gel electrode which is generally used as an standard ECG recorder.

5.5 Sample Dataset

We extracted apart from the sample ECG dataset "AliveCor's Short Single Lead ECG Recording" that is publicly available online. This dataset provides a collection of ECG amplitudes at various time scales, each representing one ECG wave, with the final column labeled as Normal and Abnormal ECGs, the latter of which includes Atrial Fibrillation. A single row looks to be an image matrix in ECG datasets, and we also know that any two categorized ECG waveforms are nearly the same; for example, one Normal ECG wave will be nearly identical to another Normal ECG wave, and one A.F. wave will be nearly identical to another A.F. wave. This is how our sample dataset appears, with the label Normal ECG and Abnormal ECG, Amplitude data ranging from -1mV to 1mV, and Time in seconds. We have a total of 2000 milliseconds in our dataset or 33.33 seconds. The dataset contains a total of 2001 columns and 8530 rows; the following Table 1 contains a sample of the dataset.

Table 1 Alivecor's single lead ECG dataset; **Description:** This table shows a sample of dataset taken from Alivecor's ECG single lead device with a label as Normal or Abnormal, each row forms a single lead ECG wave

0	1	2	3	4	5	6 ...	1999	Label
0.035032	0.037155	0.044586	0.063694	0.076433	0.085987	0.089172	-0.02229	Normal
-0.03529	-0.03257	-0.03094	-0.02986	-0.03149	-0.0342	-0.03746	0.001086	Normal
-0.30392	-0.26144	-0.22222	-0.19281	-0.17647	-0.1634	-0.14706	-0.06536	Normal
0.109467	0.117604	0.128698	0.142012	0.153107	0.161982	0.170118	0.013314	Abnormal
-0.01986	-0.01715	-0.01444	-0.01173	-0.00993	-0.00812	-0.00632	0	Abnormal
0.051136	0.0625	0.090909	0.142045	0.238636	0.335227	0.4375	0.119318	Normal
-0.12387	-0.12991	-0.13595	-0.14804	-0.16012	-0.17221	-0.18429	0.253776	Normal
-0.04615	-0.0441	-0.04205	-0.03897	-0.0359	-0.03179	-0.02769	0.019487	Abnormal
-0.02503	-0.02503	-0.02253	-0.01877	-0.01126	0.001252	0.017522	-0.0776	Abnormal
-0.07178	-0.07015	-0.06852	-0.06688	-0.06362	-0.06199	-0.05873	0.014682	Normal
-0.94677	-0.95057	-0.95437	-0.95817	-0.96198	-0.96578	-0.96578	0.235741	Normal
0.056582	0.047344	0.038106	0.025404	0.013857	0.004619	0	0.023095	Normal
-0.08696	-0.08152	-0.05978	-0.02174	0.021739	0.086957	0.173913	-0.1413	Abnormal
-0.06887	-0.13642	-0.24636	-0.39735	-0.5894	-0.81192	-1.04503	-0.08212	Normal
-0.09927	-0.1102	-0.12022	-0.12659	-0.13206	-0.13752	-0.14117	-0.03005	Abnormal
-0.44531	-0.5	-0.55078	-0.58984	-0.65625	-0.73438	-0.76172	-0.33984	Normal
-0.39799	-0.4214	-0.44816	-0.47492	-0.50836	-0.54181	-0.57525	-0.03344	Abnormal
0.027211	0.017007	0.006803	0	0	-0.0068	-0.0068	0.530612	Normal
0.632735	0.720559	0.716567	0.612774	0.327345	-0.06986	-0.48503	0.011976	Normal
0.04501	0.052838	0.086106	0.172211	0.297456	0.455969	0.632094	-0.00196	Abnormal
0.008351	0.039666	0.058455	0.075157	0.087683	0.100209	0.110647	0.096033	Normal
0.036072	0.024048	0.026052	0.048096	0.06012	0.036072	0.008016	-0.08216	Abnormal
-0.02728	-0.03104	-0.03481	-0.03763	-0.04045	-0.04327	-0.04516	0.015052	Abnormal
0.264368	0.266667	0.268966	0.268966	0.268966	0.267816	0.265517	-0.0092	Abnormal
0	-0.00084	-0.00084	-0.00168	-0.00336	-0.00419	-0.00587	-0.0302	Normal
0.086763	0.094549	0.101224	0.106785	0.113459	0.119021	0.124583	-0.02558	Normal
-0.1519	-0.15506	-0.15823	-0.16139	-0.16139	-0.16456	-0.16456	0.003165	Abnormal

6. METHODOLOGY

6.1 Objective

Our first purpose is to acquire information about the ECG and its operation, to examine the entire product offerings on the market, and to analyze what issues remain and how we may come up with a better solution, some modification, or enhancement. By analyzing the limitations and constraints of Apple's ECG watch and Sanket's 12 leads ECG, we were able to develop a portable, non-invasive point-of-care system for detecting/monitoring stress levels in various body parts of the human subject, which could be adapted to facilitate early detection of a variety of diseases or disorders related to the heart that can be correlated with an increase in stress in various body parts of the subject. Now, we can collect our own datasets and do analyses on them via the smartphone. Additionally, the data analytics section includes a forecast of whether a subject has Atrial Fibrillation or not.

6.2 Block Diagram

Below, figure (Figure 20) shows the block diagram that can be implemented on a circuit box. It should contain a total of three units, namely a Battery Unit (Power Source), a Sensing Unit, and a Wireless Communication Unit. The sensing Unit should capture leads, monitor heart rate, and process them like passing waves via various electrical circuits like amplifier or bandpass filters and denoising the final output signal. Then Analog signals are converted to digital signals and sent to Wireless Unit. Output data generated from the sensing unit should be transferred to mobile application using the wireless may be wifi/Bluetooth/internet cloud channels.

The electrical output from the heart is represented by the input analog signal, which has a voltage range of 0 mV to 3 mV and a frequency range of 0.01 Hz to 250 Hz. The output signal will contain serialized digital data translated from analog signals. The procedure can be carried out on ECG equipment; operations like filtering, amplification, and digitizing can be carried out and delivered to a PC or smartphone device. Further processing can be done to identify and anticipate different wave signals, such as QRS detection, which requires a bandwidth of 0.5Hz to 40Hz, and arrhythmia detection, which requires a bandwidth of 0.05Hz to 60Hz.

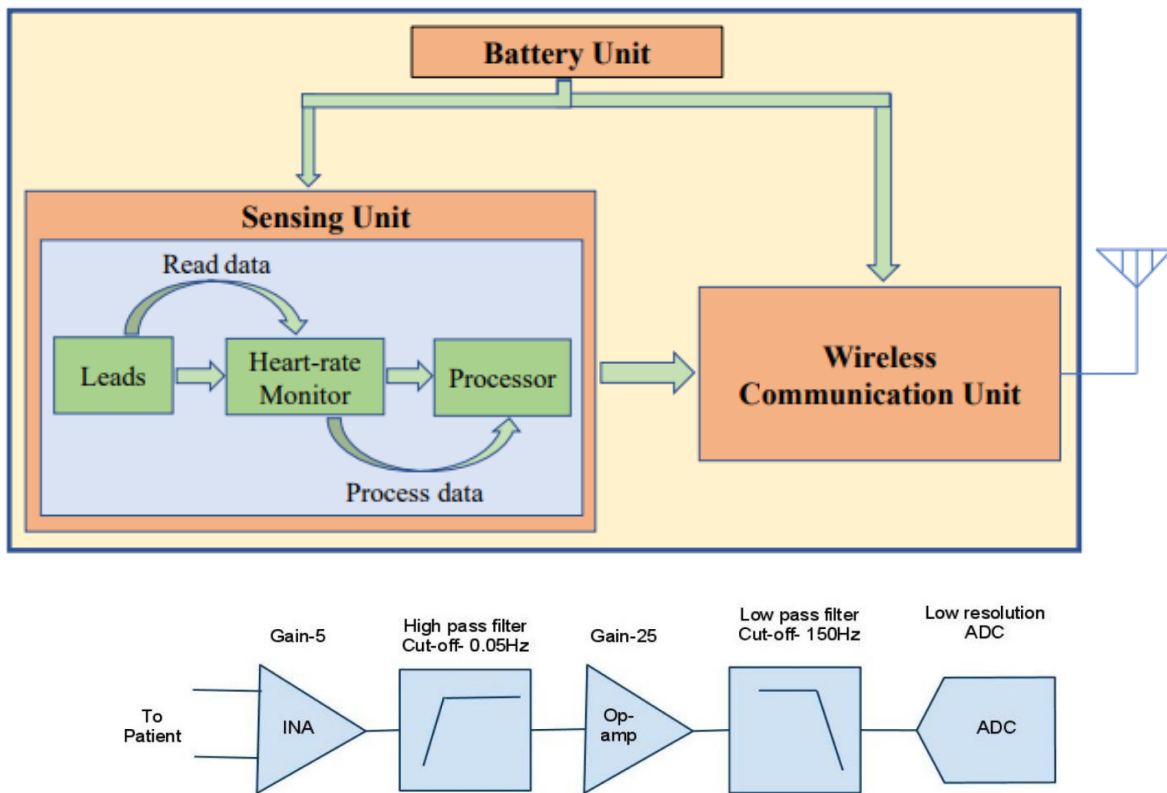


Figure 13 Block Diagram of an ECG device, **Source:** Shen, M., & Xue, S. (2015). Design and Implementation of Long-Term Single-Lead ECG Monitor. Journal of Biosciences and Medicines; **Description:** This figure shows the block diagram of an ECG device showing how the data is processed from analog to digital

Output Analog Voltage ECG signals can differ from one person to the next. An ECG's fundamental front-end device must be able to handle extremely low signals ranging from 0.5 to 5.0 millivolts. The electrode-skin contact has a direct current component of up to 300 mV, while the potential difference between the electrodes and the ground has a common-mode component of up to 1.5 V. An ECG signal's useful bandwidth varies by application, ranging from 0.5 Hz to 50 Hz for critical care unit monitoring to 1 kHz for late-potential assessments (pacemaker detection). The bandwidth of a typical clinical ECG application ranges from 0.05 Hz to 100 Hz.

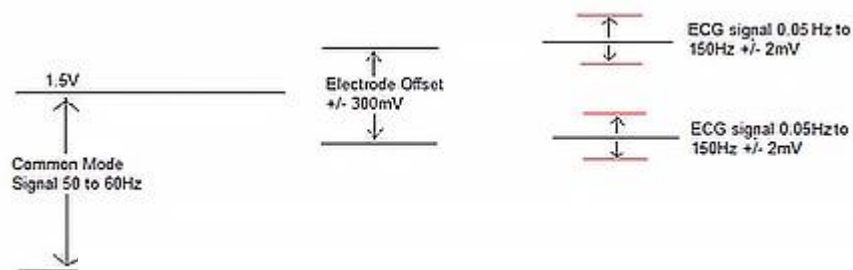


Figure 14 Working Principle of Circuit **Source:** Sharma, H., & Sharma, K. (2015). Baseline wander removal of ECG signals using Hilbert vibration decomposition; **Description:** This figure shows the voltage bandwidth gap between electrode and skin

Baseline drift is caused by patient breathing (low-frequency AC signal noise). Interference with transmission lines (50-60Hz noise from power lines). Muscle rumble (This noise is extremely difficult to eliminate because it is in the same frequency range as the genuine signal.) Typically, it is corrected in software.) Other interacting variables (i.e., radio frequency noise from other equipment). To reduce common-mode noise, we use instrumentation amplifiers with very high common-mode rejection ratios on the order of 100dB. Following the acquisition, the patient body is driven with an inverted common-mode signal, and the noise is eliminated using software methods.

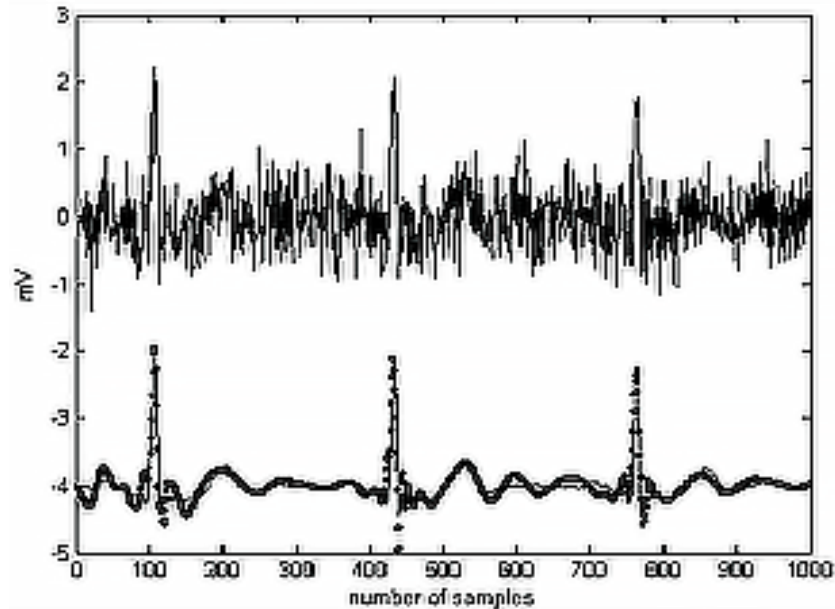


Figure 15 Noisy ECG wave; **Source:** A Novel Method to Detect Multiple Arrhythmias Based on Time-Frequency Analysis and Convolutional Neural Networks. **Description:** This figure shows the noisy and a normal ecg wave.

6.4 Circuit Diagram & Components

Below figure shows the circuit diagram of the portable non-invasive ECG device that contains two electrodes, a bypass capacitor circuit to remove D.C. noise, an amplifier circuit to amplify lower signal detection, a bandpass filter circuit to get a ranging signal, and a notch filter to remove the noise and tune it

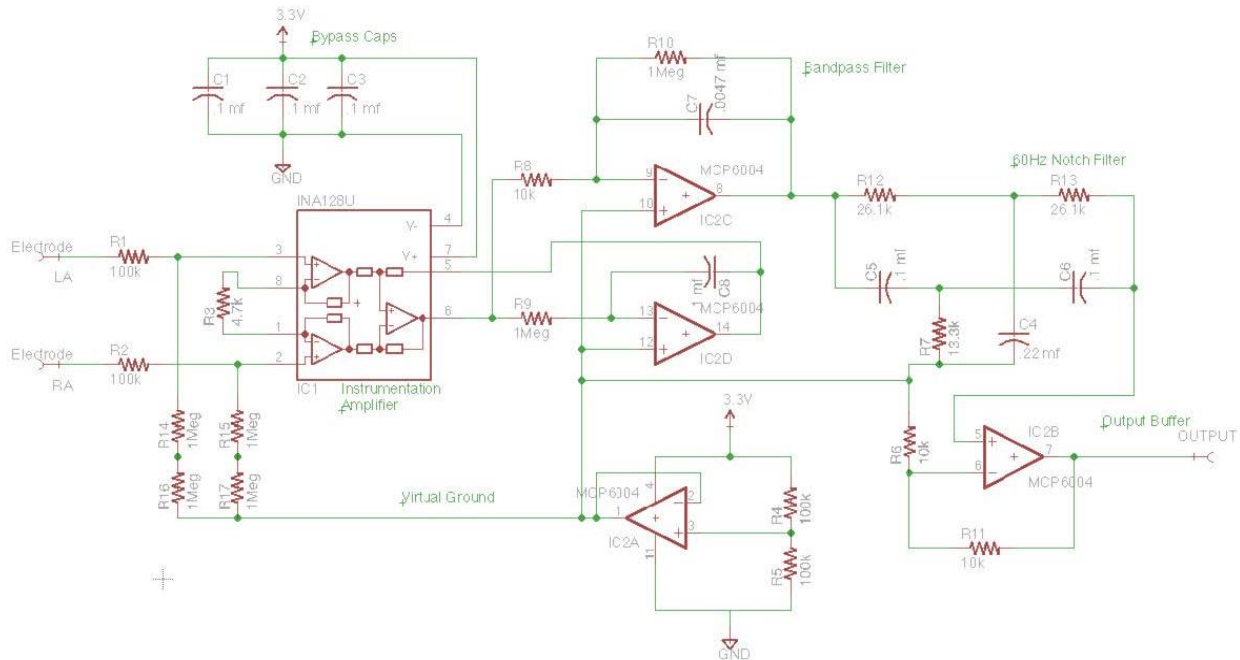


Figure 16 Circuit Diagram, **Source:** courses.cs.ishington.edu;
Description: This figure shows the ECG 2 electrode and single lead ECG recording device

These are the major components that are required to build the setup:

- **Teensy 3.2**
 - USB-based programmable microcontroller chip
 - Higher R.O.M. (64K) and Flash (256K)
 - 16 general-purpose D.M.A. channels
 - 34 digital input/output pins, 12 P.W.M. output pins
 - The output voltage of 3.3V and 5V
- **MCP6004 Low power Op-Amp**
 - It's a Quad Op-amp (14-Pin) package.
 - Input and output over the 1.8 to 6V as an operating range.
 - Gain–bandwidth product of 1 MHz with current 100 μ A.
 - 14-lead PDIP, 3.3V as the power source
- **INA128U Amplifier**
 - Amplifies the low voltage signal.
 - Low-power amplifier with high accuracy.
 - Small 3-op amp (8pins) design.



Figure 17 Teensy 3.2



Figure 18 MCP6004



Figure 19 INA128U

- **Adafruit BluefruitLE**

- Easy to add Bluetooth Low Energy connectivity
- ARM Cortex M0 core running at 16MHz
- 256KB flash memory
- 32KB SRAM
- 5V-safe inputs (Arduino Uno friendly, etc.)
- On-board 3.3V voltage regulation

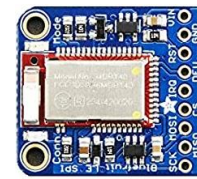


Figure 20 BlueFruit

- **Band-Pass Filter**

- Allows frequencies within a certain range
- Here range used is 1Hz to 40Hz signals are allowed

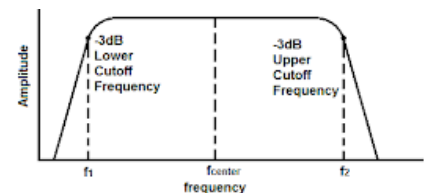


Figure 21 Band-Pass Filter

- **Notch filter**

- Band-Stop filter attenuates frequencies within a range while passing other frequencies unaltered.
- Range of frequencies is very narrow.
- Range of frequencies that are attenuated is stopband

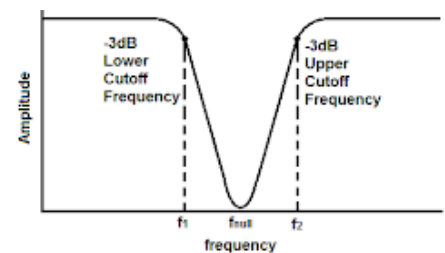


Figure 22 Notch Filter

- **Bypass Capacitor**

- It shorts A.C. signals to the ground so that any A.C. noise that may be present on a D.C. signal is removed, producing a cleaner D.C. signal.
- The value of the bypass capacitor should be at least 1/10th of the resistance across the emitter resistance, RE at the lowest frequency intended to be bypassed.

The analog output of the circuit is connected to an analog pin in teensy. The below figure 23 shows how to connect the LCD and Adafruit Bluefruit LE with Teensy 3.2.

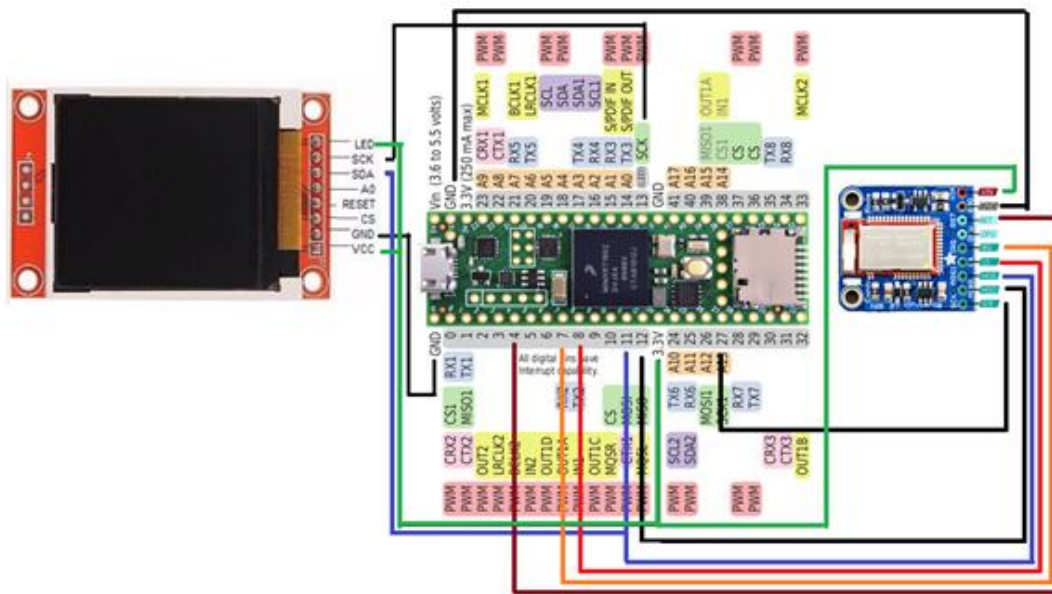


Figure 23 Circuit Diagram; **Description:** This diagram shows hardware connection of teensy, bluefruit, and LCD device

6.5 Datapoints

We may visualize the image matrix data points by plotting each row from the sample ECG dataset "AliveCor's Short Single Lead ECG Recording." We are charting Amplitude on the y-axis and Time on the x-axis, where Amplitude is between -1mV and 1mV and Time is between 0 and 2000 seconds. The following figure 24 demonstrates how a single-row plot appears.

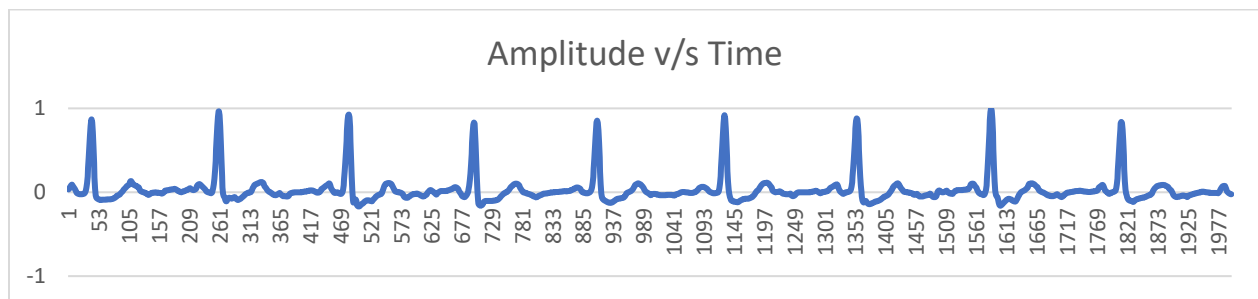


Figure 24 Sample ECG Wave Plot from the dataset; **Description:** This figure shows single lead ECG wave plotted data taken from Alivecor's Physionet database

6.6 Redefining Dataset

There were no missing data points discovered when studying the dataset. To begin, we processed the label column and changed the data points from string to boolean values of 0 and 1, where 0 denotes a normal electrocardiogram and 1 indicates atrial fibrillation. Now, to determine the skewness and bias of the data, we generated histograms of labeled columns to get insight into the data; the below histogram plot illustrates the column's occurrence of 0 and 1. In figure 18, we can see from the data points that around 58% of the data had Normal ECGs, and the remainder contained Abnormal ECGs suggesting Atrial Fibrillation. Following that, we shuffled the dataset and divided it into several pieces for training, validation, and testing.

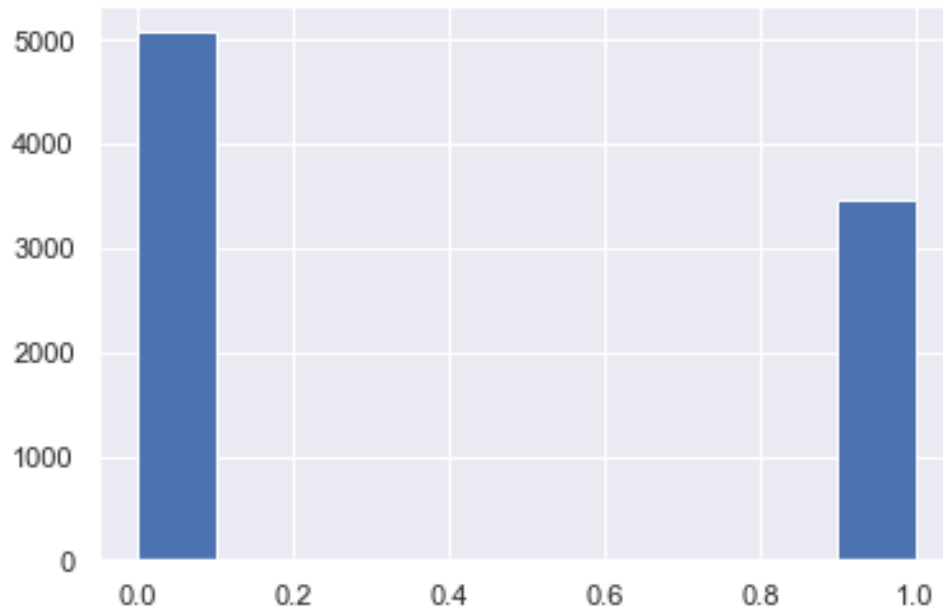


Figure 25 Histogram Normal and Abnormal ECG Occurrence;

Description: This figure shows the histogram of count of the Normal(0), and Abnormal(1) occurrence in the ECG database

6.7 Dataset Modelling and Architecture

After getting the insights into the data, we can see there is no correlation between any two columns, and every column has its own importance, so our features are the time values at which we are recording ECG with equal weights given to each column and labeled column as out predicting column. In comparison with each row as an image matrix, it seemed to be an image classification problem; now, to predict the image, we chose to build a Convolution Neural Network model (shown in figure 19) as this works better in a sharp object and edge detections techniques.

Convolutional Neural Networks (CNNs) are made up of neurons that self-optimize and learn. Each neuron will continue to accept input and perform an operation (such as a scalar product followed by a non-linear function) - the fundamental building block of an infinite number of artificial neural networks. From the input raw image vectors through the final output class score, the entire network will continue to reflect a single perceptual scoring function (the weight). The last layer will contain loss functions associated with the classes, and all of the established methodologies for traditional ANNs will remain applicable. The neurons that compose the layers of the CNN are structured in three dimensions: the input's spatial dimension (height and width) and the depth. The depth parameter does not refer to the overall number of layers in the ANN. When the activation function "ReLU" (Rectified Linear Unit) is employed, the neurons within each layer will link to only a small part of the layer preceding it.

Each ECG image is represented by a one-dimensional matrix. We divided the dataset 80% as training and 20% as a validation set. We chose a kernel size of 5; kernel size refers to the length of the one-dimensional convolution window; and our filter size ranges from 32 to 512, where filter size denotes the output space's dimensionality as we need to check different parts of the image searching for data points. We started with a model consisting of approximately nine Convolution Neural Network layers and then performed maximum pooling, dropouts, and lastly, the development of dense layers. Maximum pooling is used here to refer to a pooling process that determines the maximum or largest value in each patch of a feature map. The resulting feature maps are down-sampled or pooled to highlight the most abundant feature in the patch rather than the feature's average presence in the patch in the case of average pooling. We made use of dropouts. It is a strategy in which randomly chosen neurons are ignored during random training. This means that their contribution to the activation of downstream neurons is removed temporally during the forward trip, and any weight modifications to the neuron are skipped during the backward pass.

Neuron weights become ingrained in the network's surroundings as it learns. Specific features are assigned to neuronal weights, resulting in some specialization. Neighboring neurons become more reliant on this specialization, which can lead to a model that is overly specialized in the training data if taken too far. During training, a neuron's dependency on the context is referred to as complex co-adaptations. If neurons are discarded from the network at random during training, another neuron may be required to step in and handle the representation needed to make predictions for the absent neurons. The network is thought to learn a large number of independent internal representations as a result of this. Afterward, we utilized Adam Optimizer to make a stochastic gradient descent with a learning rate alpha of roughly 0.00006, with a total of 100 epochs and a batch size of approximately 128. Low learning rates may take a very long time to converge, whereas high learning rates may not even come close to the convergence point at all if they are used. On the basis of loss, accuracy, and precision, we evaluated our model using python libraries of TensorFlow, Keras, and Scikit-Learn.

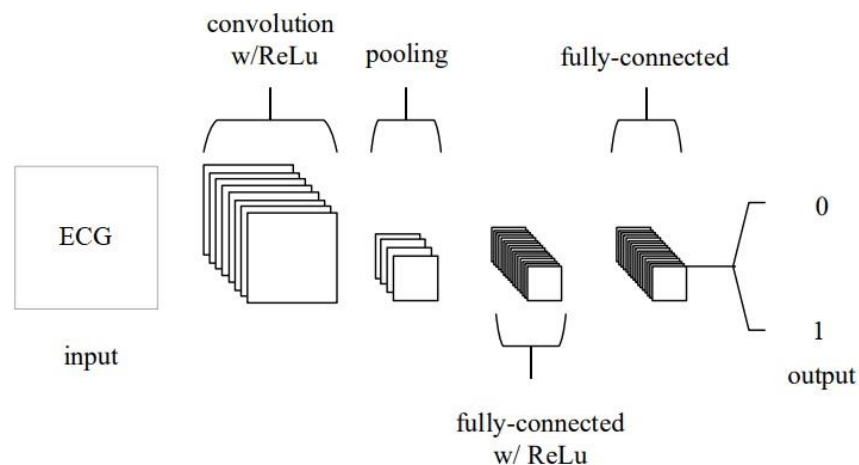


Figure 26 Convolution Neural Network; **Description:** This figure shows how the convolution neural network is working in our ECG database and providing the output as 0 (Normal) and 1 (Abnormal)

7. RESULTS AND DISCUSSION

To better represent normal and abnormal ECGs, we renamed the designated column 0 and 1, respectively, after determining that the data set is not skewed. In the end, we built a deep learning convolution neural network model using this data set. We assessed the model over the dataset after fitting and assessing our final model. We were able to get an 81.36 % accuracy. We constructed the confusion matrix and estimated the precision, recall, and F1 score after analyzing the model that is trained and tested over 100 validation epochs and 128 batch sizes. To simplify the binary classification, the x-axis displays true or false classifications with expected classifications on the other side of the matrix, while the y-axis displays the predicted classifications, as shown in figure 27 and figure 28.

		ACTUAL	
		Negative	Positive
PREDICTION	Negative	TRUE NEGATIVE	FALSE NEGATIVE
	Positive	FALSE POSITIVE	TRUE POSITIVE

Figure 27 A Sample Confusion Matrix; Description:
This figure shows a sample confusion matrix

- **True Positive** is when the model accurately predicts the positive class, i.e., when both the forecast and the observed value are positive; from the confusion matrix, we got a total of True Positive as 225.
- **True Negatives** occur when the model accurately predicts the negative class (i.e., the forecast and the observed value are both negatives); we got a total of 469 True Negatives.
- **False Positive** occurs when the model predicts the negative class incorrectly, i.e., predicted-positive for actual-negative, we got a total of 128 False Positive values.
- **False Negative** occurs when the model predicts the positive class incorrectly; that is, predicted-negative for actual-positive; we got a total of 31 False Negative values.

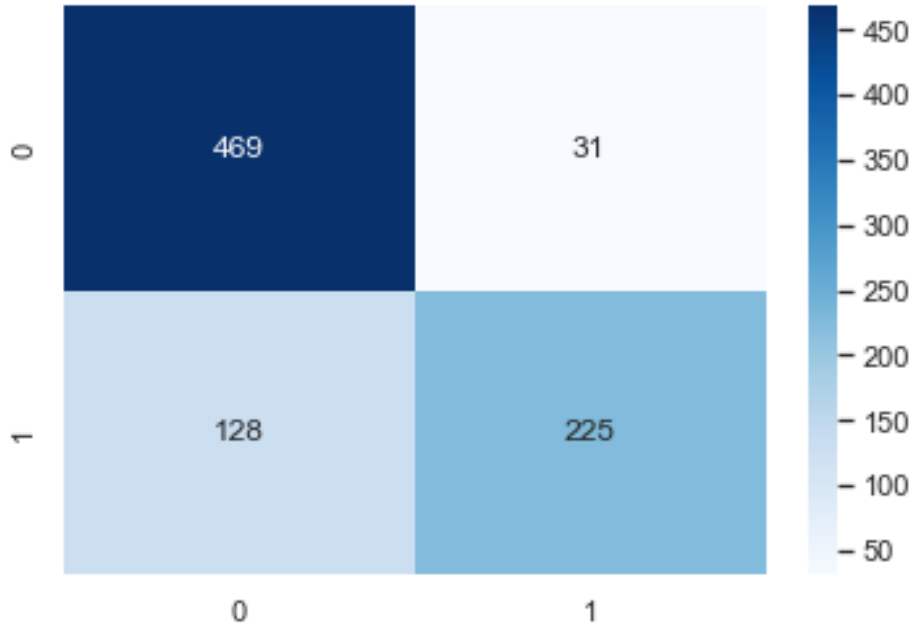


Figure 28 Confusion Matrix; **Description:** This figure shows the confusion matrix obtained after evaluating the output of the CNN model

Precision and recall are both critical for knowledge retrieval, with positive classes being more important than negative classes. Precision is defined as the percentage of truly positive predictions out of all positive predictions. Precision is a value between 0 and 1.

$$Precision = \frac{True\ Positive}{True\ Positive + False\ Positive} \quad (viii)$$

The recall is the percentage of expected positives in relation to the total Positive. We want to ensure that we do not miss any fraudulent transactions. As a result, we wish to keep False-Negative as low as possible. In these instances, we can make a trade-off between precision and recall. Similarly, we do not want to overlook any patient in the medical application. As a result, we place a premium on recall.

$$Recall = \frac{True\ Positive}{True\ Positive + False\ Negative} \quad (ix)$$

The F1 score is calculated as harmonic mean of precision and recall. It accounts for both false positives and negatives. As a result, it performs admirably on an unbalanced dataset. All three are shown in table number 2.

$$F1\ score = \frac{2 * (Precision * Recall)}{(Precision + Recall)} \quad (x)$$

Table 2 Precision, Recall & F1 score; **Description:** This table shows the calculated precision, recall, and F1 score value for the normal and atrial fibrillation on a tested dataset

	Precision	Recall	F1 score
Normal	0.79	0.94	0.86
Atrial Fibrillation	0.88	0.64	0.74

On running a total of 100 epochs over the Convolution Neural Network (CNN), the below shows the plot of the variation of loss at different epochs; here orange line denotes validation loss, and the blue line denotes training loss. For validation loss, it converges to about 28%, as shown in figures 29 and 30.

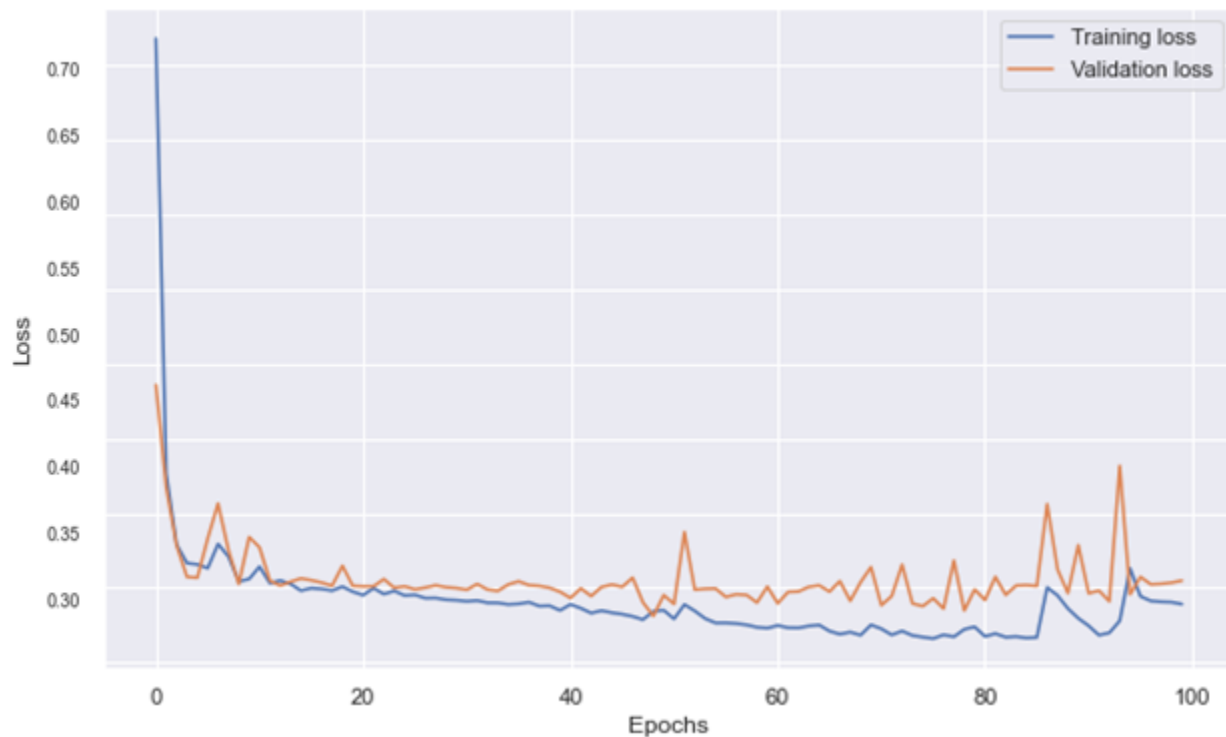


Figure 29 Loss v/s Epochs for Training Loss and Validation Loss; **Description:** This figure shows how the loss varies on the number of epochs, where the blue line shows the training loss and the orange line shows the validation loss evaluated on the convolution neural network model



Figure 30 Accuracy v/s Epochs for Training Accuracy and Validation Accuracy; **Description:** This figure shows how the accuracy varies on the number of epochs, where the blue line shows the training accuracy, and the orange line shows the validation accuracy evaluated on the convolution neural network model

The circuit diagram setup is done using the programmable chip Teensy 3.2, Bluetooth module, and the LCD device. The teensyduino and Arduino programming IDE are used to compile and execute the code. But, we were stuck at a Teensy 3.2 is out of stock everywhere, so we ordered a higher version, i.e., Teensy 4.0, to set up the circuit, but Teensy 4.0 lacked a hardware unit named “Programmable Delay Block” (PDB) which is used in reading low input signals and converting them from analog to digital. The setup and code were tried on Teensy 4.0, and input is taken using two steel plate electrodes. The data is fed into the amplifier and noise removing hardware units in order to improve the signal. Then the improved signal is converted from analog to a digital output, and this data is used to train a neural network model and tested on a given set of inputs.

9. CONCLUSIONS

Throughout this article, we've endeavored to provide a thorough overview of the procedures that must be followed when taking an ECG. The many components of the presentation were introduced, as well as the connection that existed between them. The equations and operating principles of an ECG are discussed in detail. We can draw a few conclusions from the research we've done thus far.

1. We learned how our hearts operate and how an electrocardiogram works, as well as which risk factors may be detected using an electrocardiogram. We also learned about the different types of heart disease.
2. We learned about the products that are now available on the market, as well as the need to make a move from traditional to portable devices in order to stay competitive.
3. Specifically, we looked at how a convolutional neural network can be built and how it can be used to effectively predict whether or not a person has Atrial Fibrillation with an accuracy of 81.36% and validation loss is 28%.
4. We learned how to measure the precision and recall of our model.
5. We looked into micropattern electrodes, which be used to improve the accuracy, grip, and precision of the setup in the future.
6. We learned how to assemble a complete circuit and make a product, and we developed a non-invasive portable ECG recording device.
7. Datasets were recorded and plotted and simultaneously tested on a machine learning model to detect whether the ECG detected is Normal or not.

10. FUTURE SCOPES

Following that, we can proceed to improve device configuration, implementation, and data collection. Eventually, we can get a marketable and portable, non-invasive point-of-care ECG device that will record electrocardiograms and other vital signs. More work can be done on the machine learning model to make it more efficient and can be trained on the bigger dataset. This setup can be assembled into a small portable ECG device like Sanket's ECG Device. This device can detect the abnormalities in the ECG using our convolution neural network model.

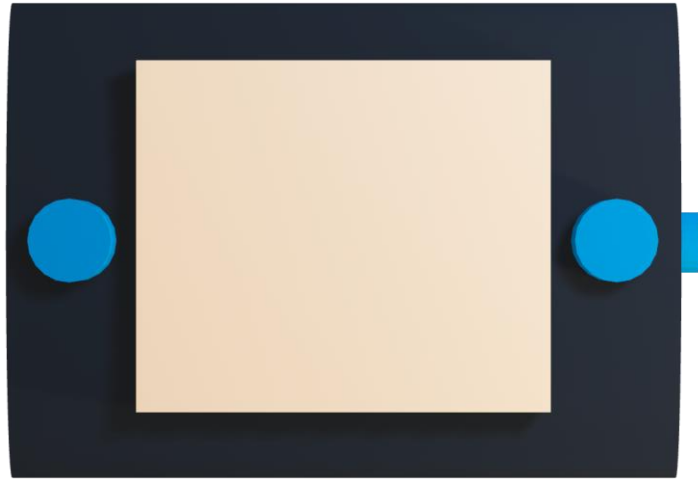


Figure 31 Prototype of ECG portable device; **Description:** This 3D object shows a prototype design of a portable ECG device that can be developed using a pcb board chip

REFERENCES

1. An, X., & Stylios, G. (2018). A Hybrid Textile Electrode for Electrocardiogram (ECG) Measurement and Motion Tracking. *Materials*, 11(10), 1887. <https://doi.org/10.3390/ma11101887>
2. Camm, A. J., Lüscher, T. F., Maurer, G., & Serruys, P. W. (Eds.). (2018). ESC CardioMed. *ESC CardioMed*. <https://doi.org/10.1093/med/9780198784906.001.0001>
3. Gargiulo, G. D. (2015). True Unipolar ECG Machine for Wilson Central Terminal Measurements. *BioMed Research International*, 2015, 1–7. <https://doi.org/10.1155/2015/586397>
4. H. Karam, E., Tashan, T., & F. Mohsin, E. (2019). Design of Model Free Sliding Mode Controller based on BBO Algorithm for Heart Rate Pacemaker. *International Journal of Modern Education and Computer Science*, 11(3), 31–37. <https://doi.org/10.5815/ijmecs.2019.03.05>
5. Haider, A., & Fazel-Rezai, R. (2014). Heart Signal Abnormality Detection Using Artificial Neural Networks1. *Journal of Medical Devices*, 8(2). <https://doi.org/10.1115/1.4027015>

6. Hong, S., Zhang, W., Sun, C., Zhou, Y., & Li, H. (2022). Practical Lessons on 12-Lead ECG Classification: Meta-Analysis of Methods From PhysioNet/Computing in Cardiology Challenge 2020. *Frontiers in Physiology*, 12. <https://doi.org/10.3389/fphys.2021.811661>
7. Husain, K., Mohd Zahid, M. S., Ul Hassan, S., Hasbullah, S., & Mandala, S. (2021). Advances of ECG Sensors from Hardware, Software and Format Interoperability Perspectives. *Electronics*, 10(2), 105. <https://doi.org/10.3390/electronics10020105>
8. Kanjilal, P., Palit, S., & Saha, G. (1997). Fetal ECG extraction from single-channel maternal ECG using singular value decomposition. *IEEE Transactions on Biomedical Engineering*, 44(1), 51–59. <https://doi.org/10.1109/10.553712>
9. Lenis, G., Pilia, N., Loewe, A., Schulze, W. H. W., & Dössel, O. (2017). Comparison of Baseline Wander Removal Techniques considering the Preservation of ST Changes in the Ischemic ECG: A Simulation Study. *Computational and Mathematical Methods in Medicine*, 2017, 1–13. <https://doi.org/10.1155/2017/9295029>
10. Madias, J. E., & Attari, M. (2004). Exercise-triggered transient R-wave enhancement and ST-segment elevation in II, III, and aVF ECG leads: a testament to the “Plasticity” of the QRS complex during ischemia. *Journal of Electrocardiology*, 37(2), 121–126. <https://doi.org/10.1016/j.jelectrocard.2004.01.009>
11. Marriott, H. J. (1964). Electrocardiographic abnormalities, conduction disorders and arrhythmias in primary myocardial disease. *Progress in Cardiovascular Diseases*, 7(2), 99–114. [https://doi.org/10.1016/s0033-0620\(64\)80013-x](https://doi.org/10.1016/s0033-0620(64)80013-x)
12. Steinberg, C., Philippon, F., Sanchez, M., Fortier-Poisson, P., O’Hara, G., Molin, F., Sarrazin, J. F., Nault, I., Blier, L., Roy, K., Plourde, B., & Champagne, J. (2019). A Novel Wearable Device for Continuous Ambulatory ECG Recording: Proof of Concept and Assessment of Signal Quality. *Biosensors*, 9(1), 17. <https://doi.org/10.3390/bios9010017>

13. Tison, G. H., Sanchez, J. M., Ballinger, B., Singh, A., Olgin, J. E., Pletcher, M. J., Vittinghoff, E., Lee, E. S., Fan, S. M., Gladstone, R. A., Mikell, C., Sohoni, N., Hsieh, J., & Marcus, G. M. (2018). Passive Detection of Atrial Fibrillation Using a Commercially Available Smartwatch. *JAMA Cardiology*, 3(5), 409. <https://doi.org/10.1001/jamacardio.2018.0136>
14. Zhou, D. X. (2020). Theory of deep convolutional neural networks: Downsampling. *Neural Networks*, 124, 319–327. <https://doi.org/10.1016/j.neunet.2020.01.018>